LBL-30810
Preprint

Lawrence Berkeley Laboratory
UNIVERSITY OF CALIFORNIA

Submitted to Physical Review Letters

Dynamics and Statistics in Multifragment Production

M. Colonna, P. Roussel-Chomaz, N. Colonna, M. Di Toro,
L.G. Moretto, and G.J. Wozniak

May 1991

NUCLEAR SCIENCE DIVISION

Prepared for the U.S. Department of Energy under Contract Number DE-AC03-76SF00098

LBL-30810

Dynamics and Statistics in Multifragment Production

M. Colonna, P. Roussel-Chomaz, N. Colonna, M. Di Toro,
L.G. Moretto, and G.J. Wozniak

Nuclear Science Division
Lawrence Berkeley Laboratory
University of California
Berkeley, Ca 94720, USA

This work was supported by the Director, Office of Energy Research, Division of Nuclear Physics of the Office of High Energy and Nuclear Physics of the U.S. Department of Energy under Contract DE-AC03-76SF00098

Dynamics and Statistics in Multifragment Production

M. Colonna [1], P. Roussel-Chomaz[2], N. Colonna, M. Di Toro[1], L.G. Moretto, and G.J. Wozniak

Nuclear Science Division, Lawrence Berkeley Laboratory, Berkeley, CA 94720

Abstract

Complex fragment production in intermediate energy heavy-ion reactions is described by coupling the dynamics of the collision stage with the subsequent statistical deexcitation stage. The simulations are compared to experimental data from the reaction $^{139}La + ^{27}Al$ at 55 MeV/u. Many of the features observed in the inclusive charge distribution, as well as in the total charge, source velocity distributions and Dalitz plots of the multifragment coincidence events are reproduced.

PACS numbers: 25.70.Np, 25.70.Gh

[1] Permanent address, INFN, L.N.S. Catania, Italy
[2] Permanent address, SEPN, CEN Saclay, 91191 Gif-sur-Yvette, Cedex, France

In contrast to lower energy reactions, intermediate energy heavy ion collisions are associated with abundant multifragment production[1,5]. Several hypotheses have been put forward to explain such a process, some involving dynamical concepts, other statistical ones. Kinetic equations, like the Landau-Vlasov, Boltzmann-Uehling-Uhlenbeck or Boltzmann-Nordheim-Vlasov equations, have been widely used to simulate the evolution of heavy-ion collisions in the intermediate energy range[6-11]. So far, these transport theories have not been able to reproduce the yields of fragments in the mass range between the projectile and target[11]. On the other hand, statistical approaches, successfully used at low energy, where complex fragments are assumed to be produced in the decay of compound nuclei formed in fusion or incomplete fusion reactions, take minimal account of entrance channel effects and cannot reproduce the non-equilibrium features observed at intermediate energy[12].

The two approaches described above are complementary and can be combined in a framework which incorporates both dynamical evolution and statistical decay. More specifically, this letter will show that the experimental charge distributions as well as the main features of the coincident events observed in a recent experiment on complex fragment production, can be reproduced by coupling a dynamical approach describing the formation of the primary fragments, to a statistical stage where these excited primary fragments can undergo any division from particle evaporation to symmetric fission.

The dynamic stage of the collision was simulated by solving the Boltzmann-Nordheim-Vlasov (BNV) equation within a test particle approach in a full ensemble method[9], each nucleon being represented by 40 test particles. The self-consistent mean field included the Coulomb potential and a nuclear potential approximated by a density dependent Skyrme-like interaction. The parameters of the latter were chosen to reproduce nuclear matter saturation properties, and a compressibility coefficient of $K = 200$ MeV. The free nucleon-nucleon cross section $\sigma_{NN}(E,\Theta)$ was used in the collision term with its energy and angular dependence. The resulting average trajectory in phase space, is followed up to a time called for the sake of convenience, the "relaxation" time. The determination of this relaxation time is of critical importance in the characterization of the primary fragments. If this time is too short the fragments are far from equilibrium, if it is too long, some part of the excitation energy and angular momentum will have already been lost by light particle evaporation. The latter is undesirable since the dynamical code does not account for all possible statistical decay channels. Thus, we have chosen the relaxation time as the time when the slope of the emitted nucleon mean energy curve changes, indicating the transition from preequilibrium emission to evaporation from a more equilibrated source.

At the relaxation time, a clustering procedure[10] is used to calculate, for each impact parameter, the primary fragment observables: mass, charge, velocity, angle, excitation energy and angular momentum. In this procedure a cluster is formed by the test particles that satisfy the relation $|r_i-r_j|<D$, where D is set to the minimum value that reproduces the mass of the target and projectile at t = 0 (D = 1.5 fm). In practice the clustering procedure may be difficult to apply at $t = t_{relaxation}$, because the fragments may not yet be well separated. Therefore, it was necessary to extend the BNV calculations to later times in order to clearly identify the clusters. Once the characteristics of the fragments are known at these later times, the time evolution of the observables is parametrized and the characteristics of the fragments at the relaxation time are obtained by back extrapolation. We have checked that the total fragment mass deduced from this method at $t = t_{relaxation}$ is within 1% of the total mass available at this time. With this method we obtain the most probable distribution of primary fragments with all their properties at the relaxation time as a function of impact parameter.

Finally, these sources are allowed to undergo sequential binary decays. The deexcitation process has been simulated with the statistical decay code GEMINI[13]. In this code, all decay channels are considered, from light particle emission to symmetric division. A Monte-Carlo technique is used to follow the decay chains of individual nuclei through sequential binary decay until the resulting products are unable to undergo further decay.

The model described above has been applied to the reaction $^{139}La + ^{27}Al$ at 55 MeV/u[14]. For the most central impact parameters (b=1,2 fm), the BNV calculations predict the occurrence of fusion accompanied by preequilibrium emission. This feature has also been observed in the Landau-Vlasov calculations[15] performed for the reaction $^{139}La + ^{12}C$ at 50 MeV/u[12] where the system fuses for all but the most peripheral impact parameters. For b = 3 fm, the mechanism observed can be characterised as fast fission. Finally the more peripheral reactions lead to a process whose features are very reminiscent of deep inelastic collisions as they are observed at low incident energy. At each impact parameter, preequilibrium emission of light particles is observed. For this very asymmetric entrance channel, the BNV calculations do not lead to three body configurations (projectile, target, fireball) at any impact parameter, contrary to more symmetric systems where a fireball is predicted[16,17].

Fig. 1 presents the mass, excitation energy, angular momentum and source velocity of the heaviest primary fragment at the end of the dynamical stage, as a function of the impact parameter. A relaxation time of 90 fm/c was chosen for this system, because this corresponds approximatively to the "kink" observed in the time evolution of the emitted nucleons' mean energy. A similar result has been reported recently by Pi et al.[15], who also found a relatively short equilibration time of 90 fm/c for the system $^{139}La + ^{12}C$ at 50 MeV/u.

A single fusion residue is observed for impact parameters below 2 fm. At 90 fm/c it has already lost about 20 nucleons by preequilibrium emission. Above b = 3 fm, two fragments are present, and are responsible for the discontinuity observed in the mass, excitation energy and angular momentum at this impact parameter. The heavy fragment mass tends toward the projectile mass for large impact parameters. The angular momentum increases up to I = 70 ħ for b = 4 fm, then decreases, due to the loss into exit channel orbital motion. Even for the most central collisions, the excitation energy remains always small compared to the total available energy in the center of mass, of 1,240 MeV, due to a strong preequilibrium emission. The importance of the preequilibrium processes at all impact parameters is one of the most striking results of the dynamical stage.

Fig. 2 shows the cross section as a function of atomic number Z for the system under study. The agreement between the data (diamonds) and the simulation (solid line with filled diamonds) throughout the entire charge distribution suggests that the approach presented in this letter correctly describes the mechanism of complex fragment production. The discrepancy observed for Z>35 may be ascribed to an underestimate of the experimental cross section due to the limited angular coverage for these forward-emitted heavy fragments. The need for a coupling of the dynamical and statistical approaches is clearly illustrated by the comparison with the result of a purely dynamical simulation presented by the dashed line, which fails completely to reproduce the experimental distribution. It should be pointed out that the cross section in the region of 15<Z<35 does not depend strongly on the choice of the relaxation time in the region of the "kink". For example, an increase of 20 fm/c in the relaxation time would lower the cross sections calculated for these fragments by only 40%. Also, the other inclusive observables of the reaction (angular distributions, emission velocities...) are reasonably well reproduced by the calculation, in both their equilibrium and non equilibrium features, as will be shown in forthcoming papers[14,17].

More severe constraints are imposed by the coincidence events. Coincident events have been separated according to the detected fragment multiplicity. A n-fold event is defined as an event where n fragments with Z≥4 are detected. Table 1 compares the different branching ratios for the binary, ternary and quaternary channels obtained from the data and the calculation after filtering through the detector acceptance. In both cases, 2-fold events represent the bulk of the detected fragments, and the branching ratios for 3-fold events agree within 20%. The underestimation of the 4-fold events in the calculation can have several origins. First, GEMINI does not take into account the deformation of the primary fragments at the end of the dynamical stage, which can affect the branching ratios of the different decay channels. Furthermore, the BNV code does not include any dynamical fluctuations[8,18-20] and therefore can not produce any multifragment effect which might arise from such fluctuations, in presence of dynamical instabilities.

The experimental total charge and source velocity distributions with the corresponding theoretical quantities obtained from the calculations after filtering through our detection efficiency, are shown in Fig. 3. The overall agreement is quite satisfactory. The peak position in the Z_{tot} distribution for the 2-fold events is well reproduced. For the 3-fold events, the peak position obtained in the calculation is somewhat larger than the data. The tail at low Z_{tot} observed in the data for the 2 and 3-fold events, which corresponds to higher n-fold events where only 2 or 3 fragments are detected, is underestimated in the calculation. These two effects are a consequence of the underestimate of the 4 and higher n-fold events in the simulation. The shift observed in the Z_{tot} peak position may also be due to an underestimate of the excitation energy deposited in the primary sources. The source velocity plotted in the right-hand column of Fig. 3 has been obtained with the relation $v_s=\Sigma m_i v_i/\Sigma m_i$, where m_i and v_i are the masses and velocities of the detected or filtered fragments. These source velocity distributions are gated for $Z_{tot}\geq30$, in order to reduce to a reasonable level the contamination arising from incompletely detected events and to avoid biasing our kinematical reconstructions. For all types of events, the position of the calculated peak is in good agreement with the data, but the width is underestimated for 3 and 4-fold events.

The 3-body decay features are best shown by means of Dalitz plots. In this representation, each three-fold event is represented as a point for which the distances to the sides of the triangle indicate the values Z_1/Z_{tot}, Z_2/Z_{tot}, Z_3/Z_{tot}. In the Dalitz plots presented here, the distributions have been symmetrized by randomly assigning Z_1, Z_2, Z_3. A gate has also been applied to the total detected charge ($Z_{tot}>30$). Fig. 4 compares the data with the results of the "BNV+Gemini" calculation before and after filtering. It should be stressed that at the end of the dynamical stage the Dalitz plot would be empty, since only either an incomplete fusion residue or a target and projectile remnant are produced. After the deexcitation stage, the simulated Dalitz plot is very similar to the data, with a predominance of events with one heavy and two light fragments. The relative abundance of these events located in the corners of the triangle is considerably reduced after filtering through our detection efficiency, because the heavy fragments are strongly forward peaked and very often do not pass through the filter.

In this letter we have presented an attempt to reproduce the non-equilibrium and equilibrium features of complex fragments emission in intermediate energy heavy ion reactions by coupling a kinetic description of the dynamical stage of the collision with a subsequent statistical decay of the primary sources. The dynamical evolution of the ^{139}La + ^{27}Al reaction at 55 MeV/u has been simulated by solving the BNV equation up to a relaxation time when the characteristics of the primary fragments have been extracted and introduced as input in the statistical code GEMINI. The overall agreement obtained between the simulation and the data for the charge distributions, as well as the total charge, source velocity distributions and Dalitz plots indicates that such a "dynamical-statistical" coupling is a powerful tool for the understanding of the complex fragment production mechanisms. Some discrepancies are observed for high multiplicity events that could be ascribed to multifragment processes.

The authors wish to thank A. Bonasera and F. Gulminelli for providing the clustering program used in the calculations, and Ph. Chomaz for very helpful discussions. They also thank all the people who participated in the experiment with the 55 MeV/u ^{139}La beam: Y. Blumenfeld, S. Bradley, D.N. Delis, B. Libby, H. Madani, A. Marchetti, M.A. McMahan, A. Mignerey, J.C. Meng, G.F. Peaslee and Q. Sui. This work was supported by the Director, Office of Energy Research, Office of High Energy and Nuclear Physics, Division of Nuclear Physics, of the U.S. Department of Energy under Contract No. DE-AC03-76SF00098.

References

[1]- Y. Blumenfeld et al., Phys. Rev. Lett. **66** (1991) 576

[2]- D.R. Bowman, BAPS Vol. **36** (1991) 1332

[3]- R. Trockel et al., Phys. Rev. C **39** (1989) 729

[4]- R. Bougault et al., Phys. Lett. B **232** (1989) 291

[5]- Y.D. Kim et al., Phys. Rev. Lett. **63** (1989) 494

[6]- Ch. Gregoire et al., Nucl. Phys. **A465** (1987) 315

[7]- H. Stöcker and W. Greiner, Phys. Rep. **137** (1986) 277

[8]- G.F. Bertsch and S. Das Gupta, Phys. Rep. **160** (1988) 190 and references therein

[9]- A. Bonasera, G.F. Burgio, M. Di Toro, Phys. Lett. B **221** (1989) 233
A. Bonasera, G. Russo, H.H. Wolter, Phys. Lett. B **246** (1990) 337

[10]- A. Bonasera et al., Phys. Lett. B **244** (1990) 169

[11]- A. Adorno et al., Nucl. Phys. A in press

[12]- D.R. Bowman et al., Nucl. Phys. **A523** (1991) 386

[13]- R.J. Charity et al., Nucl. Phys. **A483** (1988) 371

[14]- P. Roussel-Chomaz et al., in preparation

[15]- M. Pi, E. Suraud and P. Schuck, Nucl. Phys. **A524** (1991) 537

[16]- B. Borderie, M.F. Rivet and L. Tassan-Got, Ann. Phys. Fr. **15** (1990) 287 and references therein

[17]- M. Colonna et al., in preparation

[18]- Ph. Chomaz, G.F. Burgio, and J. Randrup, Phys. Lett. B **254** (1991) 340

[19]- S. Ayik and Ch. Gregoire, Nucl. Phys. **A513** (1990) 187

[20]- J. Randrup and B. Remaud, Nucl. Phys. **A514** (1990) 339

Table 1 : Comparison of the experimental and calculated proportions of multifragment events. A gate has been set on the total detected charge ($Z_{tot}\geq30$).

	2-fold/Total	3-fold/Total	4-fold/Total
Data	0.869	0.122	0.0088
Simulation	0.855	0.144	0.0017

Figure Captions

Fig.1 : Evolution as a function of impact parameter (b) of the excitation energy (E*), angular momentum (I), source velocity (V_s) and mass (A_s) of the heaviest fragment produced in the BNV calculation at t = 90 fm/c for the system ^{139}La + ^{27}Al at 55 MeV/u.

Fig. 2 : Comparison of the experimental and calculated charge distribution for the system ^{139}La + ^{27}Al at 55 MeV/u. No normalization factor has been applied to the simulation. The statistical errors on experimental data are smaller than the diamonds and the errors related to the extraction procedure are smaller than 20% except above Z=35 where the cross section can be underestimated by up to 60% due to the reduced angular coverage for the heavy fragments.

Fig. 3 : Comparison of the experimental (solid line) and calculated (dashed line) total charge (left-hand column) and source velocity (right-hand column) distributions for different fragment multiplicities in the case of ^{139}La + ^{27}Al at 55 MeV/u. The spectra have been normalized to the same maximum.

Fig. 4 : Comparison of the linear contour Dalitz plots obtained from the data and from the simulation before and after filtering through the detection efficiency, for the system ^{139}La + ^{27}Al at 55 MeV/u.

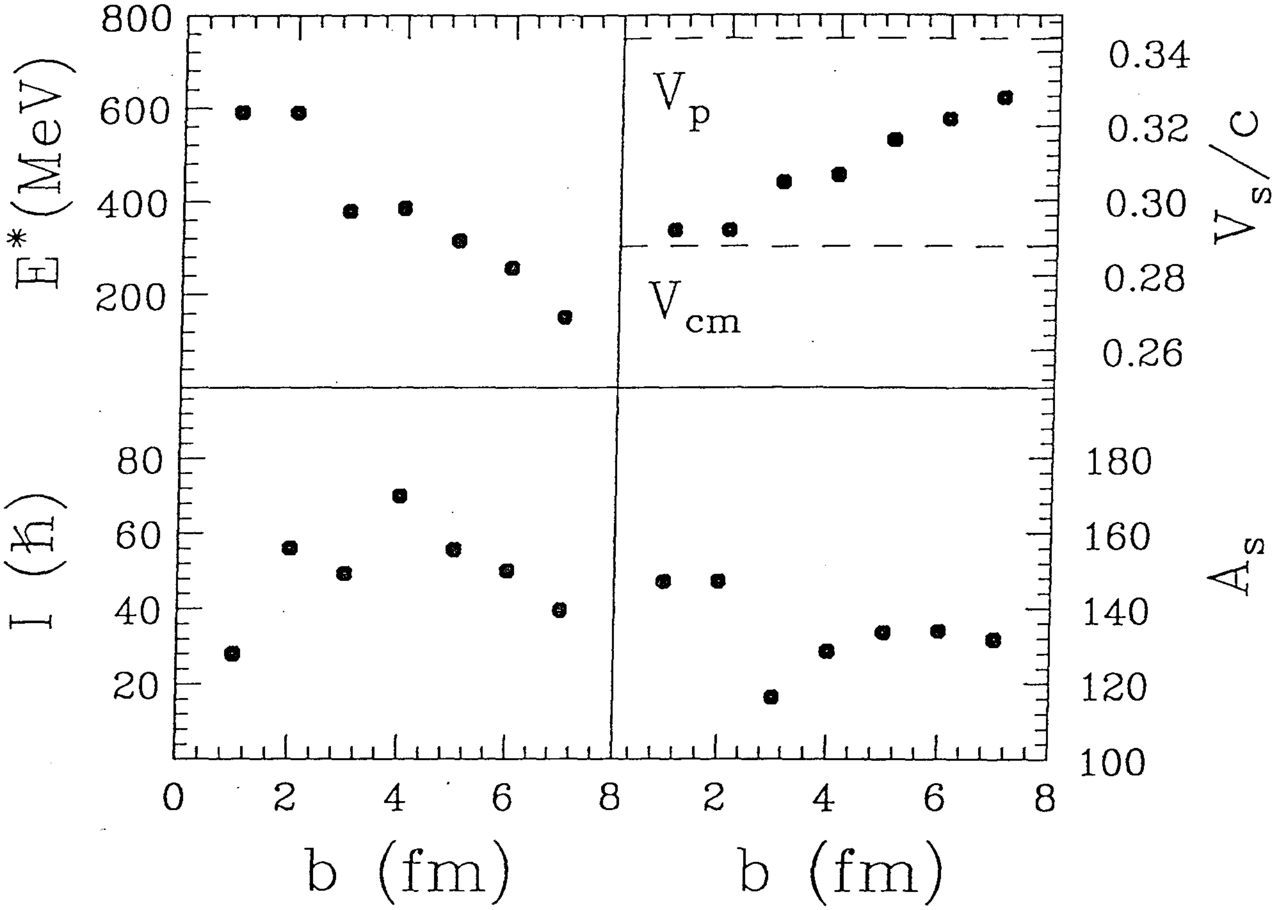
800
600
400
200
E*(MeV)
0.34
0.32
0.30
0.28
0.26
V_s/c
V_p
V_{cm}
80
60
40
20
I (ħ)
180
160
140
120
100
A_s
0
2
4
6
8
b (fm)
b (fm)

Figure 1

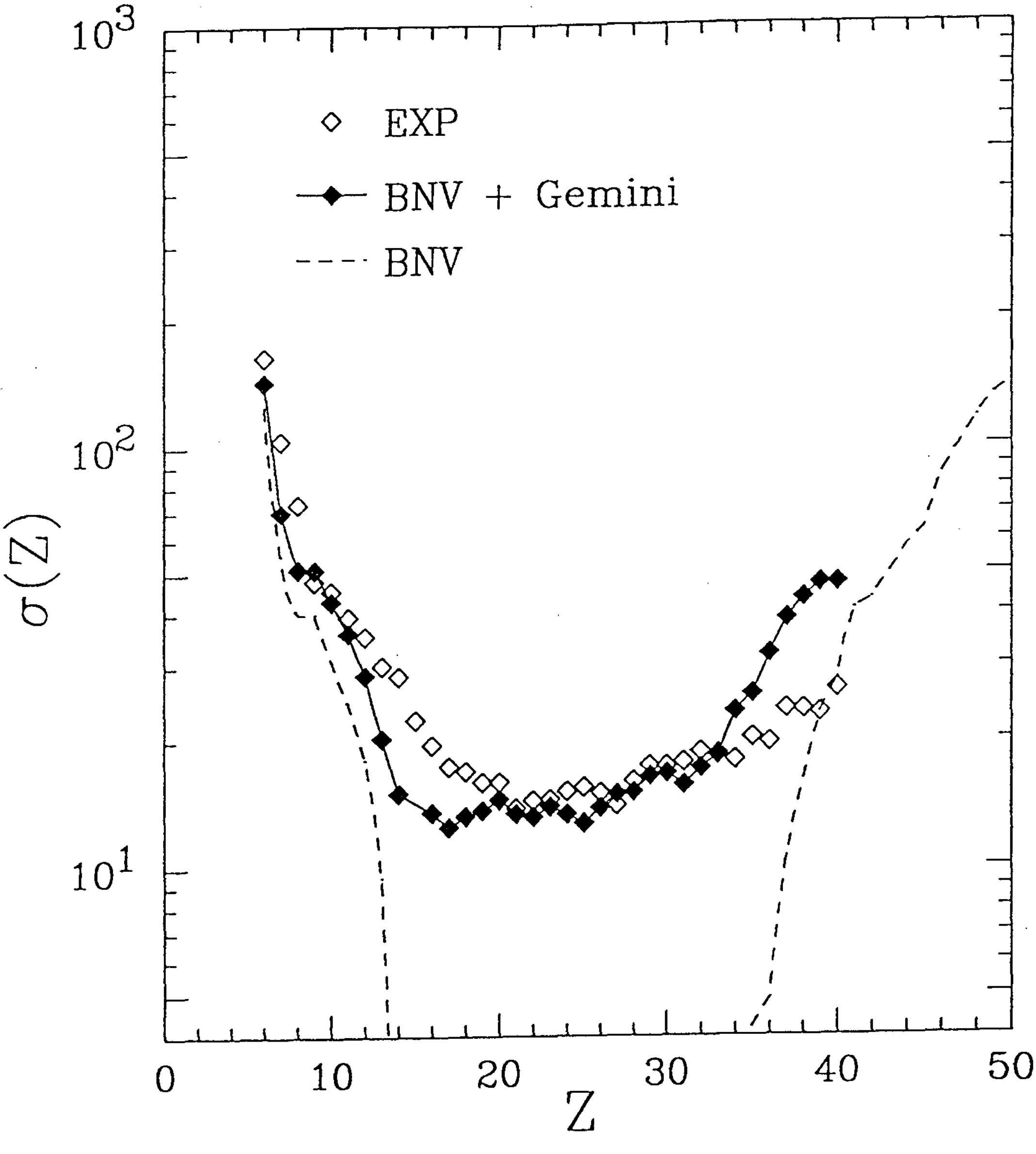

Figure 2

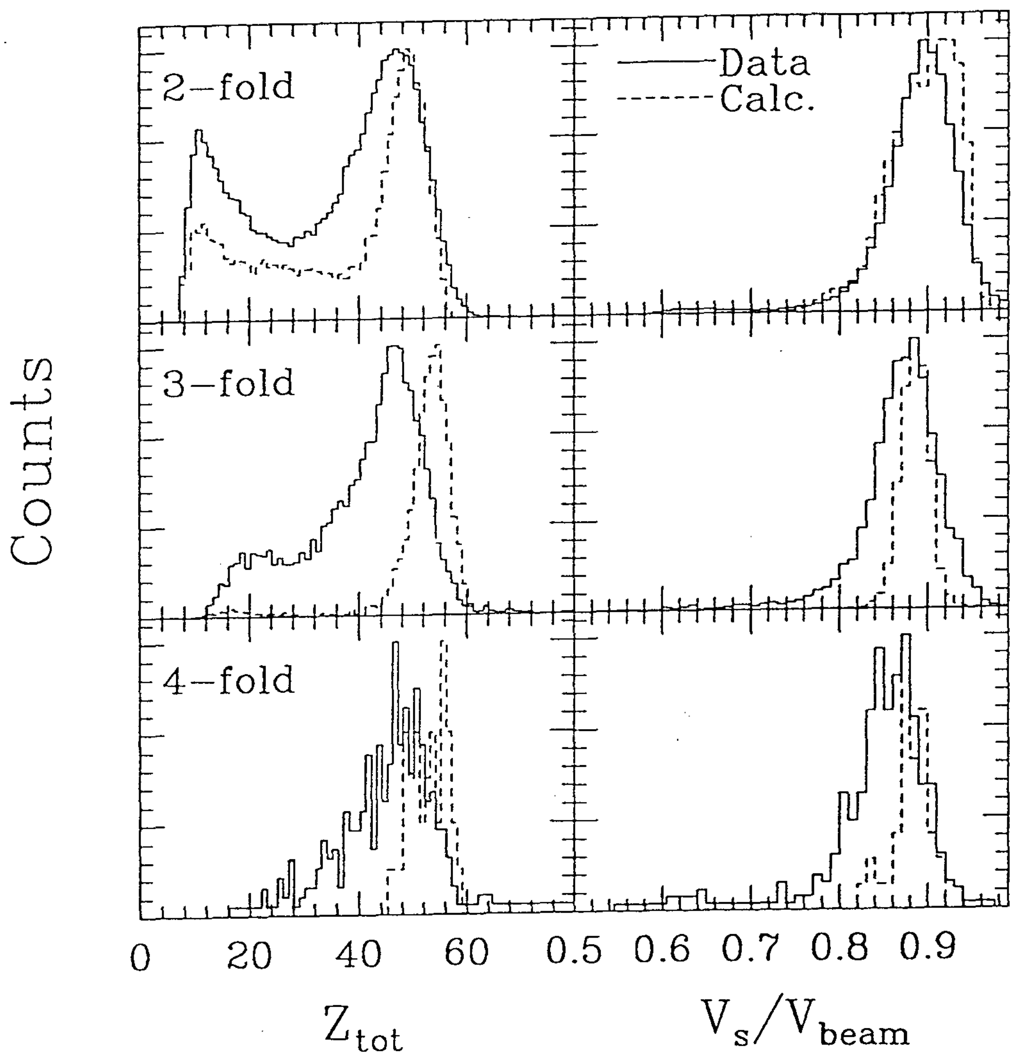
Counts
2—fold
3—fold
4—fold
Data
Calc.
0
20
40
60
0.5
0.6
0.7
0.8
0.9
Z_{tot}
V_s/V_{beam}

Figure 3

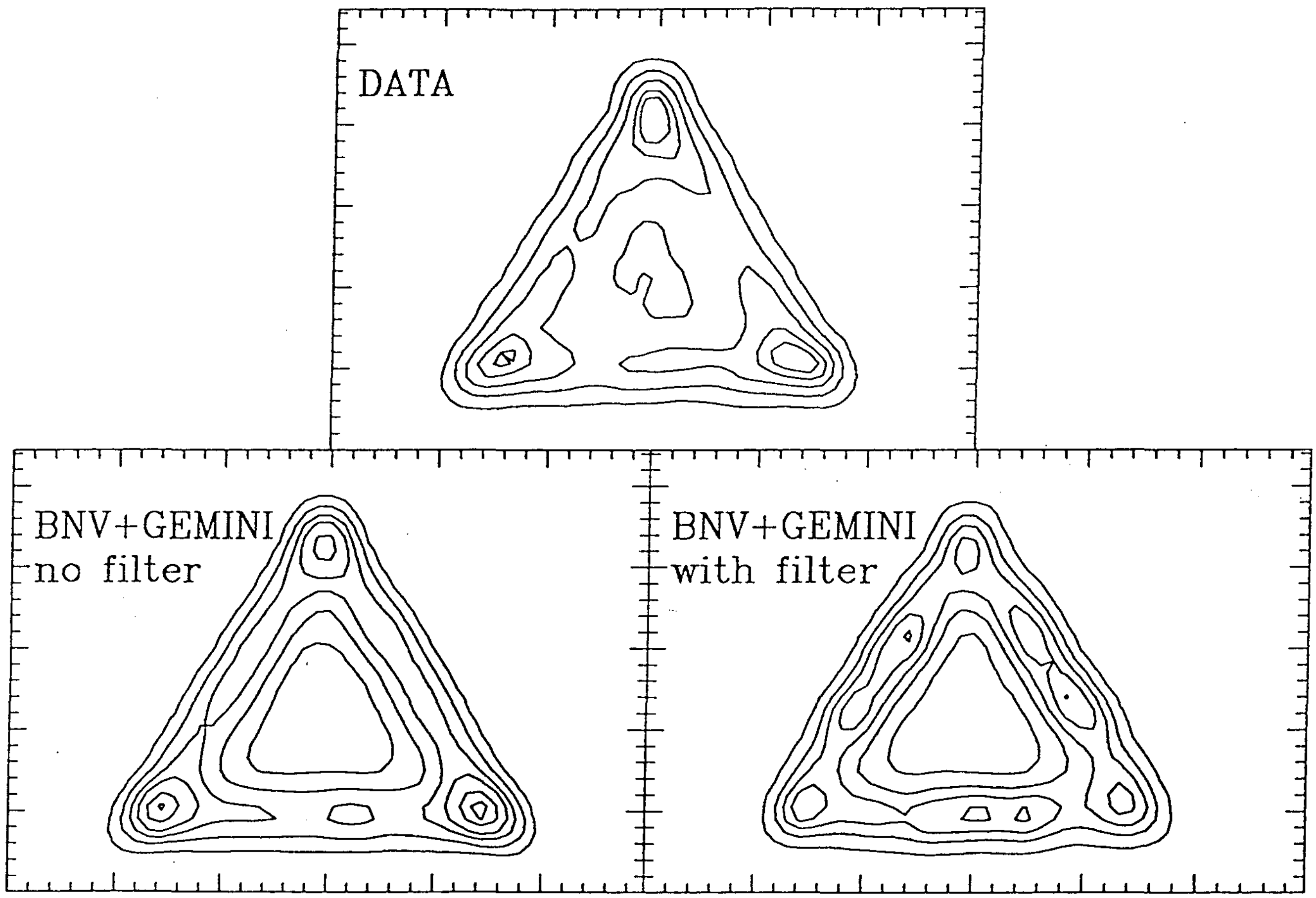

Figure 4